International Symposium
On Turbulence and Shear Flow
Phenomena (TSFP-9)
June 30 - July 3, 2015 *Melbourne, Australia*

MODELLING OF TURBULENT ENERGY FLUX IN CANONICAL SHOCK-TURBULENCE INTERACTION

Russell Quadros, Krishnendu Sinha
Department of Aerospace Engineering
Indian Institute of Technology Bombay
Mumbai, India 400076

Johan Larsson
Department of Mechanical Engineering
University of Maryland, College Park
MD 20742, USA

ABSTRACT

Supersonic and hypersonic flows often encounter high heat loads due to presence of shock waves. The unclosed turbulent energy flux correlation in the mean energy conservation equation significantly affects the heat transfer rate. In conventional RANS models, which are based on gradient diffusion hypothesis, it is modelled in terms of turbulent conductivity and gradient of mean temperature. This modelling approach often overpredicts the value of energy flux in the region of the shock. In the current work, we first apply the conventional and realizable model to predict the turbulent energy flux in canonical shock-turbulence interaction. The shortcomings of these models in predicting the energy flux across the shock are highlighted, and a differential equation model is proposed based on linear theory. The results obtained are compared with available direct numerical simulation data and a good match is found for turbulent energy flux generation across a shock. Finally, for its ease of implementation, an algebraic model is proposed with the aid of linear theory that predicts the turbulent energy flux correctly across the shock for a range of upstream Mach numbers.

1 INTRODUCTION

High-speed flows in aerospace applications have shock waves interacting with boundary layers in different parts of the vehicle surface and in engine components. Such shock/boundary-layer interactions (SBLI) are often marked by high localized surface pressure and heat transfer rates. Predicting the heating loads is especially important in supersonic and hypersonic applications with turbulent boundary layers. Majority of the existing turbulence models for heat flux prediction yield acceptable results in boundary-layer flows (Bowersox, 2009), but their predictive capability is severely limited in shock-dominated flows (Roy & Blottner, 2001).

An important unclosed term in the mean energy conservation equation, which governs the heat transfer rate, is the turbulent energy flux vector $\widetilde{u_j''e''}$. Here, u_j'' represents the velocity fluctuation in the j^{th} direction, e'' represents the internal energy fluctuation and tilde represents Favre averaging. Conventionally, this term is modelled as a product of turbulent conductivity and gradient of mean temperature. Turbulent conductivity is related to the eddy viscosity μ_T via a turbulent Prandtl number Pr_t. A constant value of $Pr_t = 0.89$ gives satisfactory result in flat plate boundary layers and is often used in SBLI configurations. This modelling approach however overpredicts the actual wall heat transfer rate significantly in SBLI.

An alternate model based on variable Pr_t approach is proposed by Xiao *et al.* (2007). It solves additional differential equations for enthalpy variance and its dissipation rate, and employs these two quantities in the formulation of turbulent heat flux vector. In shock-dominated flows, this approach leads to improved wall heat flux predictions, yet it overpredicts experimental data. To the best of our knowledge, there is no direct study which involves modelling of the turbulent energy flux across the shock. An effort in this direction is the work by Bowersox (2009) which proposes an algebraic model for the turbulent energy flux in supersonic flows, but is limited to zero-pressure-gradient boundary layers without shock waves.

In a recent work, Quadros *et al.* (2015) present a detailed study of the turbulent energy flux at a shock wave. They investigate the physical processes that govern the generation of energy flux correlation in a canonical shock-turbulence interaction (STI). This model problem consists of a homogeneous isotropic turbulence which is purely vortical in nature being carried by a one-dimensional uniform mean flow passing through a nominally normal shock wave. The turbulence is amplified by the shock, and the shock in turn gets distorted. Schematic of this problem is shown in figure 1. This is possibly the simplest configuration that isolates the effect of shock on turbulence without other effects such as boundary-layer gradient, flow separation and streamline curvature. Inspite of its geometrical simplicity, STI displays a range of physical effects such as turbu-

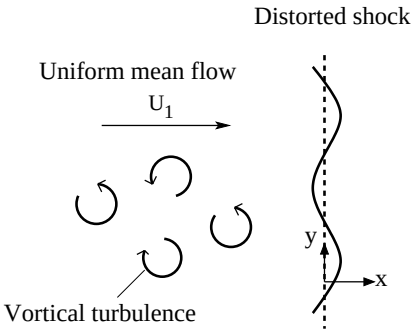

Figure 1. Schematic showing a shock wave distorted upon interaction with turbulent fluctuations.

lence anisotropy, generation of acoustic waves, baroclinic torques, and un-steady shock oscillations.

The work presented in Quadros *et al.* (2015) relies primarily on linear interaction analysis (LIA), a theoretical approach to analyse canonical STI. The analysis involves solving the fundamental interaction of a single two-dimensional plane wave with a shock which generates downstream disturbances that can be characterised in terms of Kovasznay modes of vorticity, entropy and acoustic. Integration over a specified upstream turbulence spectrum yields three-dimensional turbulence statistics downstream of the shock. The LIA results obtained for energy flux are compared with direct numerical simulation (DNS) data available from Larsson *et al.* (2013). A good match is found between LIA and DNS data in predicting some of the key physics of the interaction.

As part of modelling the turbulent energy flux in shock-turbulence interaction, Quadros *et al.* (2015) identify the mechanisms contributing to turbulent energy flux generation based on linearised Rankine-Hugoniot conditions which are valid for small upstream fluctuations. The dominant terms are further modelled based on LIA results. The resulting differential equation for turbulent energy flux is solved along with the k and ε equation to give the jump across the shock as well as the downstream decay. A good match in the streamwise evolution is found upon comparison with the DNS data for a range of upstream Mach numbers. However, it is to be noted that including an additional differential equation for energy flux may require significant modification in the existing computational fluid dynamics (CFD) codes. For their ease of implementation, algebraic heat flux models are preferred in CFD, and are in use in most Reynolds-averaged Navier-Stokes (RANS) simulations.

In this paper, we apply existing turbulence models to predict the turbulent heat flux generated at a shock wave. These include conventional eddy viscosity model and realizable model. A variant of the previously modelled differential equation for the turbulent energy flux is also presented. These model predictions are evaluated against linear theory results and available DNS data. Finally, we develop a new algebraic model to accurately predict the energy flux generated in shock-turbulence interaction.

2 TURBULENT ENERGY FLUX IN SHOCK-TURBULENCE INTERACTION

Quadros *et al.* (2015) studied the generation of turbulent energy flux in the canonical STI problem using LIA,

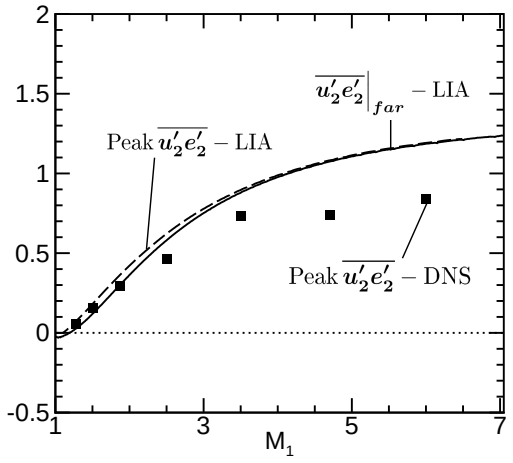

Figure 2. Variation of $\overline{u_2'e_2'}$ with upstream Mach number. The velocity fluctuation is normalized by the upstream mean velocity and the energy fluctuation is normalized by the downstream mean temperature and the specific gas constant R. All correlations are further normalized by the upstream TKE.

M_1	M_t	Re_λ	$R_{kk}/(2U_1^2)$
1.28	0.15	40	7.3×10^{-3}
1.50	0.15	40	5.3×10^{-3}
1.87	0.22	40	6.9×10^{-3}
2.50	0.22	40	4.0×10^{-3}
3.50	0.22	40	2.1×10^{-3}
4.70	0.23	40	1.2×10^{-3}
6.00	0.23	40	0.7×10^{-3}

Table 1. List of the DNS cases from Larsson *et al.* (2013) with the listed parameters corresponding to the location just upstream of the shock.

which models the upstream turbulence as a collection of planar waves. Each of these waves is considered to independently interact with the shock. The governing equations downstream of the shock are linearized Euler equations and the jump in fluctuations across the shock is determined by linearized Rankine-Hugoniot conditions. A set of linear algebraic equations are obtained by substituting the planar waveforms into the governing equations. Solving these equations yields the disturbance field downstream of the shock for a given upstream vortical wave. The downstream turbulent field for a full three-dimensional upstream turbulence is obtained by integrating the two-dimensional planar wave results over a specified energy spectrum. Details of this analysis can be found in Mahesh *et al.* (1996).

DNS of canonical STI was carried out by Larsson *et al.* (2013) for a vortical turbulence passing through a normal shock. Table 1 shows the cases from the DNS analysis whose data is utilized in the current study. The Mach numbers range from low supersonic to hypersonic limit. The turbulent Mach number M_t and the Reynolds number based on

Taylor scale Re_λ for each of the cases are also listed. Here, turbulent Mach number is defined as $M_t = \sqrt{R_{kk}}/\tilde{a}$, where R_{kk} represents twice the turbulent kinetic energy, and $\tilde{a}$ represents the Favre averaged speed of sound. Re_λ is given by $\overline{\rho}\sqrt{R_{kk}/3}\lambda/\overline{\mu}$, where λ is the Taylor scale and $\overline{\mu}$ is the average dynamic viscosity.

The turbulent energy flux values upstream of the shock are zero as the turbulence is vortical in nature and void of temperature fluctuations. However, just downstream of the shock, both LIA and DNS predict a peak positive energy flux. Further downstream, DNS shows a steep decrease in the energy flux values to negligible levels whereas LIA predicts a constant far-field value. The peak values of energy flux as predicted by both DNS and LIA for varying Mach numbers are shown in figure 2 (reproduced from Quadros *et al.* (2015)). Also shown is the far-field value of LIA, and at high Mach numbers, it is almost equal to the LIA peak energy flux. Note that conventional Reynolds averaging/fluctuation is used instead of its Favre counterpart, as negligible difference is observed upon comparison using the DNS data set. The peak energy flux as per theory matches well with DNS for low Mach numbers upto $M_1 < 2$, with the theory overpredicting the values at higher shock strengths. The LIA prediction reaches an asymptotic value of 1.32 at high Mach numbers, while DNS shows a limiting value less than 1. Overall, a good qualitative match is observed between LIA and DNS indicating that the key physical mechanisms governing the energy flux transport are captured by the theory.

It is important for any model that aims to predict the turbulent energy flux results, to capture this peak positive value. Quadros *et al.* (2015) formulated a differential equation-based model, that for a given Mach number, captures the corresponding peak positive value and the acoustic decay that follows. A good match with DNS data was obtained for a range of upstream Mach numbers, and a slight variant of this model is discussed in this work. However, greater emphasis is laid in the current study on the development of an algebraic model due to its ease of implementation in comparison with the differential equation-based model.

3 MODELLING OF TURBULENT ENERGY FLUX

3.1 Conventional Modelling

The turbulent energy flux is conventionally modelled using gradient diffusion hypothesis as

$$\overline{u'e'} = -\frac{\kappa_T}{\overline{\rho}}\frac{\partial \overline{T}}{\partial x}, \tag{1}$$

where $\overline{\rho}$ and $\overline{T}$ are the mean density and temperature. Thermal conductivity κ_T is given by $\kappa_T = \mu_T C_v/Pr_T$, where C_v is the specific heat at constant volume and Pr_T represents the turbulent Prandtl number having a constant value of 0.89. Eddy viscosity is given by $\mu_T = C_\mu^0 \overline{\rho} k^2/\varepsilon$, where $C_\mu^0 = 0.09$, k is the turbulent kinetic energy (TKE) and ε is the dissipation rate of TKE. In order to compute for the turbulent energy flux in the given model problem, the mean flow variables are prescribed as hyperbolic tangent profiles across the shock, with the shock thickness obtained from DNS data. The values of k and ε used in expression for eddy viscosity are obtained by solving the corresponding differential equations (Sinha *et al.*, 2003) using a fourth order Runge-Kutta method with the inlet boundary values specified from the DNS data. The resulting values for k and ε match well with DNS as reported in earlier works (Sinha *et al.*, 2003; Sinha, 2012).

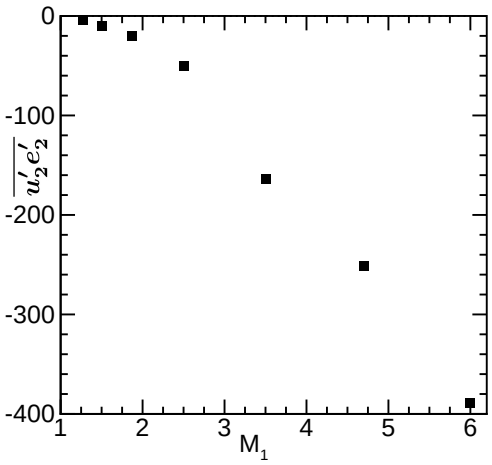

Figure 3. Peak $\overline{u_2'e_2'}$ values for varying upstream Mach numbers as predicted by conventional model with the shock-thickness taken from the DNS data. Note that the peak $\overline{u_2'e_2'}$ increases without bound as the shock-thickness is decreased, as it would be in an actual CFD simulation during grid-refinement. The results correspond to turbulent Mach number $M_t = 0.15$ just before the shock. Normalisation as described in figure 2.

The value of energy flux obtained using (1) is zero in the region upstream and downstream of the shock due to uniform mean flow temperature on either sides of the normal shock. However, the energy flux assumes a peak negative value in the region of the shock, and the peak values obtained for a range of upstream Mach number are highlighted in figure 3. In the limit of $M_1 \to 1$, the value of energy flux predicted by the model reduces to zero, and with increasing Mach number, the magnitude of the negative peak rises to a value that is almost two orders of magnitude higher than the post-shock DNS predictions. Also, in a CFD framework, this formulation yields a grid-dependent value of energy flux in the region of the shock, and increasing the grid point density further increases the magnitude of the negative peak.

3.2 REALIZABLE MODEL

In the canonical shock-turbulence interaction, the Reynolds stress as predicted by the conventional model is given by (Sinha *et al.*, 2003)

$$\overline{\rho u'u'} = -\frac{4}{3}\mu_T\frac{\partial \overline{u}}{\partial x} + \frac{2}{3}\overline{\rho}k. \tag{2}$$

This modelling approach leads to uphysically high values of TKE in the region of shock due to its proportionality with the mean velocity gradient. The realizability correction limits the value of eddy viscosity in the region of shock through the form $C_\mu = \min(C_\mu^o, \sqrt{C_\mu^o}/s)$ (Thivet *et al.*, 2001), where $s = S/(\varepsilon/k)$, $S = \sqrt{(2S_{ij}S_{ji} - (2/3)S_{kk}^2)}$ and

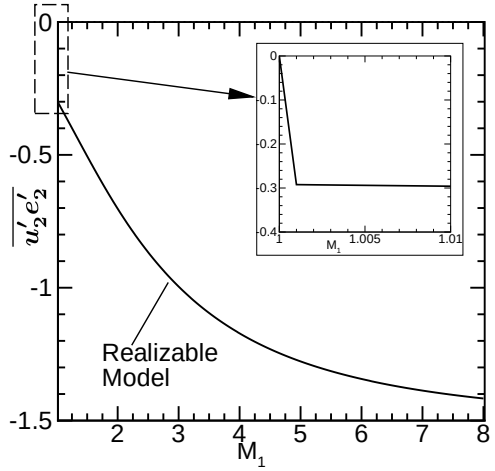

Figure 4. Variation of peak $\overline{u_2'e_2'}$ with upstream Mach number as predicted by realizable model with shock thickness taken from the DNS data. The peak value is independent of the shock thickness, which is indicative of a grid-independent solution in a CFD simulation. Normalisation as described in figure 2.

$S_{ij} = 1/2(\partial\overline{u}_i/\partial x_j + \partial\overline{u}_j/\partial x_i)$. In the region of high gradients such as shock $C_\mu = (\sqrt{c_\mu^o}\varepsilon)/(Sk)$ and therefore

$$\mu_T = \frac{\sqrt{3C_\mu^o}}{2}\frac{\overline{\rho}k}{\left|\frac{\partial\overline{u}}{\partial x}\right|}. \tag{3}$$

Thus the expression for energy flux given by (1) reduces to

$$\overline{u'e'} = -\frac{\sqrt{3C_\mu^0}}{2}\frac{kC_v}{Pr_T\left|\frac{\partial\overline{u}}{\partial x}\right|}\frac{\partial\overline{T}}{\partial x} \tag{4}$$

in the shock region.

The value of TKE as well as the mean variables required for the above formulation are obtained as described in the previous section. Similar to the conventional model, the realizable model yields a zero value of energy flux outside the region of shock. However, inside the shock region, a peak negative value is obtained as per (4). This peak energy flux value for varying Mach number is plotted in figure 4. For almost all Mach numbers, the realizable model predicts a negative energy flux in the shock region but the magnitude is restricted due to the realizability constraint, and is of the same order as the post-shock DNS value. Contrary to the eddy viscosity formulation, the realizability limiter yields a peak $\overline{u_2'e_2'}$ which is independent of the shock thickness assumed i.e., in a real CFD simulation, this peak value in the shock region will be insensitive to grid refinement. In the limit of $M_1 \to 1$, the realizable model switches to the conventional model formulation and predicts a value of zero energy flux as shown in the inset figure. In the limit of $M_1 \to \infty$, the model saturates to a negative limiting value, a trend similar to the DNS data but opposite in sign.

3.3 Differential Equation-Based Model

The equation for the conservation of total enthalpy across the shock wave can be written in terms of the shock-normal component u_n as

$$\frac{\partial h}{\partial x} + u_n\frac{\partial u_n}{\partial x} = 0. \tag{5}$$

For an unsteady distorted shock wave of the form presented in figure 1, $u_n \simeq \overline{u} + u' - \xi_t$, which assumes small deviation of the shock wave from its mean location. Linearising the above equation in terms of fluctuations in enthalpy h' and streamwise velocity u', we get

$$\frac{\partial h'}{\partial x} + \overline{u}\frac{\partial u'}{\partial x} + u'\frac{\partial\overline{u}}{\partial x} - \xi_t\frac{\partial\overline{u}}{\partial x} = 0 \tag{6}$$

Taking a moment with u' and Reynolds averaging yields a differential equation for the energy flux correlation.

$$\gamma\frac{\partial}{\partial x}\overline{u'e'} = -\overline{u'^2}\frac{\partial\overline{u}}{\partial x} + \overline{u'\xi_t}\frac{\partial\overline{u}}{\partial x} - \overline{u}\frac{\partial}{\partial x}\frac{\overline{u'^2}}{2} + \overline{h'\frac{\partial u'}{\partial x}} \tag{7}$$

where the enthalpy fluctuations are replaced by the internal energy fluctuations via $h' = \gamma e'$. The first term on the RHS represents generation of turbulent energy flux due to mean compression in the shock wave, and the second term brings in the corresponding shock-unsteadiness effect. The change in the streamwise Reynolds stress across the shock contributes to the turbulent energy flux via the third term on the RHS. The last term is a correlation of the enthalpy fluctuations with the change in the streamwise velocity fluctuations across the shock.

The first two source terms are analogous to the production and the shock-unsteadiness damping terms in the TKE equation presented in Sinha *et al.* (2003). We follow their modelling approach to write $\overline{u'\xi_t} = b_1\overline{u'^2}$, which is based on the assumption that the unsteady shock oscillations are caused by the incoming velocity fluctuations. The streamwise Reynolds stress is then closed in terms of the turbulent kinetic energy by considering its isotropic form i.e., $\overline{u'^2} = (2/3)k$ (Sinha *et al.*, 2003). The last term is dropped from the equation for want of an adequate closure approximation. The final model equation for the turbulent energy flux thus takes the form

$$\frac{\partial}{\partial x}\left(\overline{u'e'}\right) = -c_0 k\frac{\partial\overline{u}}{\partial x} - c_1\overline{u}\frac{\partial k}{\partial x} \tag{8}$$

where $c_0 = 2(1-b_1)/(3\gamma)$, $b_1 = 0.4 + 0.6\exp(2(1-M_1))$ and $c_1 = 1/(3\gamma)$. The first model term in the above equation generates a positive turbulent energy flux across the shock wave, while the second term leads to a negative contribution to the energy flux correlation.

Now consider the differential equation governing the jump in TKE at the shock is given by (Sinha *et al.*, 2003)

$$\overline{\rho}\overline{u}\frac{\partial k}{\partial x} = -\frac{2}{3}\overline{\rho}k\frac{\partial\overline{u}}{\partial x}(1-b_1) \tag{9}$$

Also, from the mean energy conservation equation across the shock, we can write

$$\overline{u}\left|\frac{\partial\overline{u}}{\partial x}\right| = C_p\frac{\partial\overline{T}}{\partial x}. \tag{10}$$

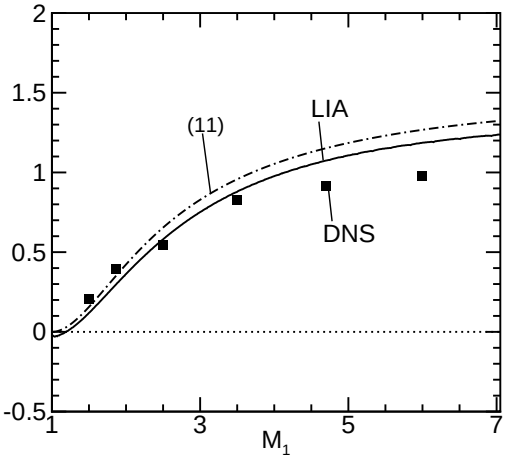

Figure 5. Variation of $\overline{u_2' e_2'}$ with upstream Mach number as predicted by (11). Also shown are the corresponding DNS values extrapolated to shock center and far-field LIA results. Normalisation as described in figure 2.

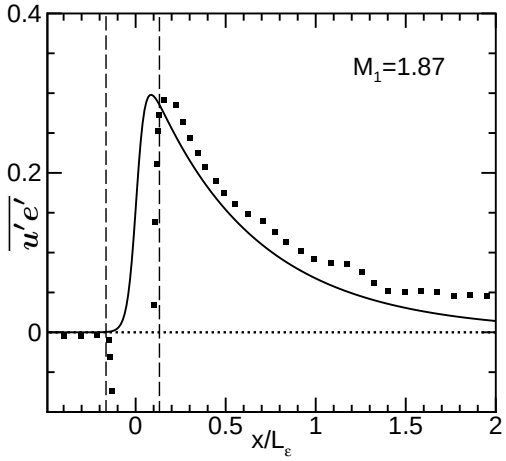

Figure 6. Variation of $\overline{u'e'}$ along streamwise direction as per (12) (line) and DNS (symbol) for the case of $M_1 = 1.87$. The vertical lines near $x/L_\varepsilon = 0$ represent the mean shock thickness. Normalisation as described in figure 2.

Using the above two equations, (8) can be written as

$$\frac{\partial}{\partial x}\left(\overline{u'e'}\right) = c_{ue}\left(\frac{k}{\overline{u}}\right) C_p \frac{\partial \overline{T}}{\partial x} \tag{11}$$

where $c_{ue} = c_o - (2/3)c_1(1-b_1)$. This equation is compact with only one modelled term governing the value of energy flux across the shock. Moreover, similar to conventional form, the energy flux is expressed in terms of gradient in mean temperature.

Figure 5 shows the energy flux values as predicted by (11) for varying upstream Mach numbers. Also shown are the downstream DNS values of energy flux extrapolated to the shock center and the far-field LIA results. $\overline{u'e'}$ attains a value of zero as $M_1 \to 1$ and saturates to a positive limiting value at high Mach numbers similar to the DNS and LIA results. A good match is seen with the LIA results, and the model slightly overpredicts as compared to the DNS data.

The acoustic mode is dominant in the region just behind the shock (Quadros *et al.*, 2015). The decay of the energy flux following the positive peak is largely affected by this mode. This decay can be modelled in terms of the dissipation length scale $L_\varepsilon = k^{(3/2)}/\varepsilon$, which is representative of the large acoustic scales in the turbulence field. The full transport equation for energy flux takes the following form

$$\frac{\partial}{\partial x}\left(\overline{u'e'}\right) = c_{ue}\left(\frac{k}{\overline{u}}\right) C_p \frac{\partial \overline{T}}{\partial x} - c_2 \frac{\overline{u'e'}}{L_\varepsilon} \tag{12}$$

where $c_2 = 0.3 + 3\exp(1-M_1)$ is a Mach number dependent modelling constant which is found to match the DNS data well.

Figure 6 shows the streamwise variation of energy flux for the case of $M_1 = 1.87$ obtained by numerically integrating (12). The shock is located at $x = 0$ and the corresponding DNS mean shock thickness is shown using two vertical lines. The model predicts a zero value of energy flux upstream of the shock with a peak positive value obtained across the shock, which matches with the corresponding DNS trend. The downstream acoustic decay is captured well qualitatively, with the model slightly underpredicting the energy flux values along streamwise direction as compared to the DNS data.

3.4 Proposed Algebraic Model

To overcome complexities involved in implementing an additional differential equation in an existing CFD solver, we propose an algebraic model for the turbulent energy flux at the shock as

$$\overline{u'e'} = \beta \frac{kC_v}{\left|\frac{\partial \overline{u}}{\partial x}\right|} \frac{\partial \overline{T}}{\partial x} \tag{13}$$

This form is similar to the realizablity constraint shown in (3) with β here as an unknown modelling parameter. Using (10), the above equation can be written as

$$\overline{u'e'} = \frac{\beta k \overline{u}}{\gamma}, \tag{14}$$

where the turbulent energy correlation is seen to be proportional to the turbulent kinetic energy. This is physically consistent with linear theory results that show all correlations generated across the shock to be directly proportional to the upstream TKE.

Further, the normalised expression for energy flux can be written as

$$\overline{u'e'}|_{Norm.} = \frac{\overline{u'e'}}{R\overline{u}_1 \overline{T}_2 \frac{k_1}{\overline{u}_1^2}}. \tag{15}$$

Using (14) with the upstream values of k and U along with (15), the expression can be simplified to

$$\overline{u'e'}|_{Norm.} = \beta \frac{M_1^2}{T_r}, \tag{16}$$

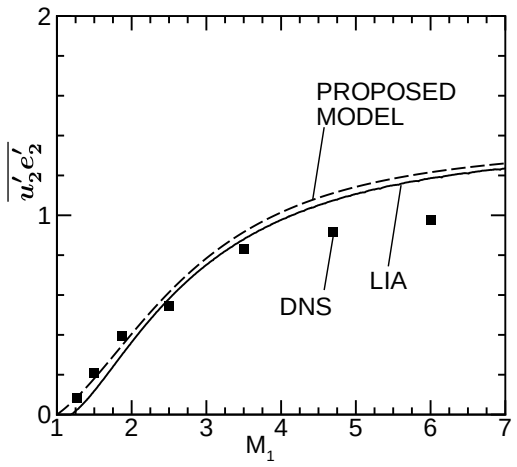

Figure 7. Variation of $\overline{u_2' e_2'}$ with upstream Mach number as per new algebraic formulation. Also seen are the DNS values of energy flux extrapolated to the shock center and the far-field LIA results.

where T_r is the ratio between the downstream and the upstream mean temperature. In the high Mach number regime, this ratio is proportional to M_1^2, and the above expression saturates to a limiting value

$$\overline{u'e'}|_{Norm.} = \beta \frac{(\gamma+1)^2}{2\gamma(\gamma-1)}. \tag{17}$$

A similar trend is seen in both the DNS and LIA results at high Mach numbers as explained earlier in figure 2. In order to find out the value of modelling parameter β, we equate (17) to the LIA far-field limiting value of 1.38.This gives a value of $\beta = 0.27$ for $\gamma = 1.4$. However, in the limit of $M_1 \to 1$, the energy flux attains this value of β which is physically incorrect. On the contrary, the energy flux predicted by the conventional model in the $M_1 \to 1$ limit is zero (as $\overline{u'e'}$ is proportional to the mean temperature gradient) which is consistent with the DNS and LIA predictions. We therefore propose a low Mach number correction of the form

$$\beta' = (1 - e^{1-M_1})\beta, \tag{18}$$

which yields $\beta' = 0$ as $M_1 \to 1$ and $\beta' \to \beta$ as $M_1 \to \infty$.

Figure 7 shows the model predictions of energy flux for a range of upstream Mach numbers. Also shown in the figure are the downstream DNS values of energy flux extrapolated to the shock center and the far-field LIA values. The model matches well with DNS for $M_1 < 2$, and for higher Mach numbers, it is close to LIA and slightly overpredicts the DNS values.

4 CONCLUSION

In this paper, we look at various modelling strategies to predict the turbulent energy flux generated in a canonical shock-turbulence interaction. Application of conventional $k-\varepsilon$ models based on gradient diffusion hypothesis yields large negative value of energy flux in the shock region, which rises drastically with increasing Mach numbers. These values are much higher in magnitude than the post-shock DNS predictions which yield a low positive energy flux. Realizable model also predicts peak negative values of the energy flux in the shock region but the peak value is limited by the realizability constraint. A differential equation model based on linear interaction analysis is formulated that provides a good estimate of turbulent energy flux generated across the shock as well as the downstream acoustic decay. Finally, for its ease of implementation, an algebraic model is developed based on linear theory, and it gives a good match for amplification in energy flux across the shock for varying Mach numbers.

ACKNOWLEDGEMENTS

The first author wishes to acknowledge Vishnu Goodwill, a graduate student under the supervision of the second author, for useful discussions. The first and second authors would like to thank Indian Space Research Organisation-Space Technology Cell (ISRO-STC) and Aeronautics Research and Development Board (ARDB) for supporting this research.

REFERENCES

Bowersox, R. D. W. 2009 Extension of equilibrium turbulent heat flux models to high-speed shear flows. *J. Fluid Mech.* **633**, 61–70.

Larsson, J., Bermejo-Moreno, I. & Lele, S. K. 2013 Reynolds- and Mach number effects in canonical shock-turbulence interaction. *J. Fluid Mech.* **717**, 293–321.

Mahesh, K., Lele, S. K. & Moin, P. 1996 The interaction of a shock wave with a turbulent shear flow. *Tech. Rep.* 69. Thermosciences division, Department of Mechanical Engineering, Stanford University, Stanford, CA.

Quadros, R., Sinha, K. & Larsson, J. 2015 Turbulent energy flux generated by shock/vortical-turbulence interaction. *To be submitted to J. Fluid Mech.* .

Roy, C. J. & Blottner, F. G. 2001 Review and assessment of turbulence models for hypersonic flows. *Progress in Aerospace Sciences* **42 (7)**, 469–530.

Sinha, K. 2012 Evolution of enstrophy in shock/homogeneous turbulence interaction. *J. Fluid Mech.* **707**, 74–110.

Sinha, K., Mahesh, K. & Candler, G. V. 2003 Modeling shock-unsteadiness in shock-turbulence interaction. *Phys. Fluids* **15**, 2290–2297.

Thivet, F., Knight, D. D., Zheltovodov, A. A. & Maksimov, A. I. 2001 Importance of limiting the turbulent stresses to predict 3D shock-wave/boundary-layer interactions. *23rd International Symposium on Shock Waves, Fort Worth, TX* .

Xiao, X., Hassan, H. A., Edwards, J. R. & Jr., R. L. Gaffney 2007 Role of turbulent Prandtl numbers on heat flux at hypersonic Mach numbers. *AIAA Journal* **45 (4)**, 806–813.